PAPER • OPEN ACCESS

Fast Frequency and Phase Lock of Grid-connected TGS Based on FIR Filter

View the article online for updates and enhancements.

Fast Frequency and Phase Lock of Grid-connected TGS Based on FIR Filter

F Ji[1, 2] and J Xu[1]

Faculty of Science and Engineering, University of Nottingham Ningbo China, Ningbo 315000, China

E-mail: Feng.Ji@nottingham.edu.cn

Abstract. The thermoelectric generation system (TGS) has many advantages such as clean, no mechanical vibration and high reliability. When TGS is connected to the power grid, it requires that the frequency and phase are same as the power grid. It will take a number of working periods for the response time under the traditional method. A frequency and phase lock method with FIR filter will be introduced in the paper. It is based on the Capture and EPWM module of TMS320F28335. The phase lock can be carried out in one period. And the working frequency of TMS320F28335 is 150MHZ. Therefore, the speed of the whole operation is fast. The experimental results show that the method is feasible.

1. Introduction

Because of the advantages of high working frequency (150MHZ), fast operation speed and abundant integrated peripheral resources (including EPWM, CAPTURE, ADC modules), TMS320F28335 is suitable for the core controller of TGS which works on the grid-on mode. In this project, TMS320F28335 is used to quickly capture and calculate the frequency and phase value of the power grid by using the Capture module. The parameter of the EPWM can be adjusted immediately according to the calculation results. Therefore, the output waveform of the inverter which is driven by EPWM module will be in the same frequency and phase with the power grid.

The work of the paper is focused on the design and test of the experiment platform for TGS. The basic control strategy of frequency and phase lock has been described. The AC sampling circuit is used to collect the power grid signal. The zero-crossing comparison circuit is used to convert the signal into the square waveform signal with the same frequency and phase. The Capture module of TMS320F28335 is used to record and calculate the frequency and phase of the square waveform. The corresponding frequency and phase of the EPWM signal are generated according to the calculation results. The EPWM signal is used to drive the full bridge inverter circuit to generate sinusoidal waveform with the same frequency and phase as the power grid. The LCD1602 which is based on the SPI of TMS320F28335 is also introduced in detail [1-3].

As shown in the Figure 1, the power grid voltage can be sampled. Then the sampling signal is converted into the corresponding zero-crossing pulse waveform. The zero-crossing pulse is

connected to the pin of the CAPTURUE module of TMS320F28335. Therefore, the real-time frequency and phase of the power grid can be measured and calculated. The calculated power grid frequency and phase are directly used as the reference value in the SPWM program. Based on this, the corresponding SPWM pulse is generated by the EPWM module of TMS320F28335. The SPWM signal is used to drive the full bridge circuit to generate the AC waveform which has the same frequency and phase as the power grid.

When the frequency or phase of the power grid changes during operation, the system can detect the frequency and phase in one period. Then the output waveform can be adjusted to be the same frequency and phase with the power grid in the second period. And the working frequency of the TMS320F28335 is 150MHZ. Therefore, the speed of frequency and phase lock is very fast [4-6].
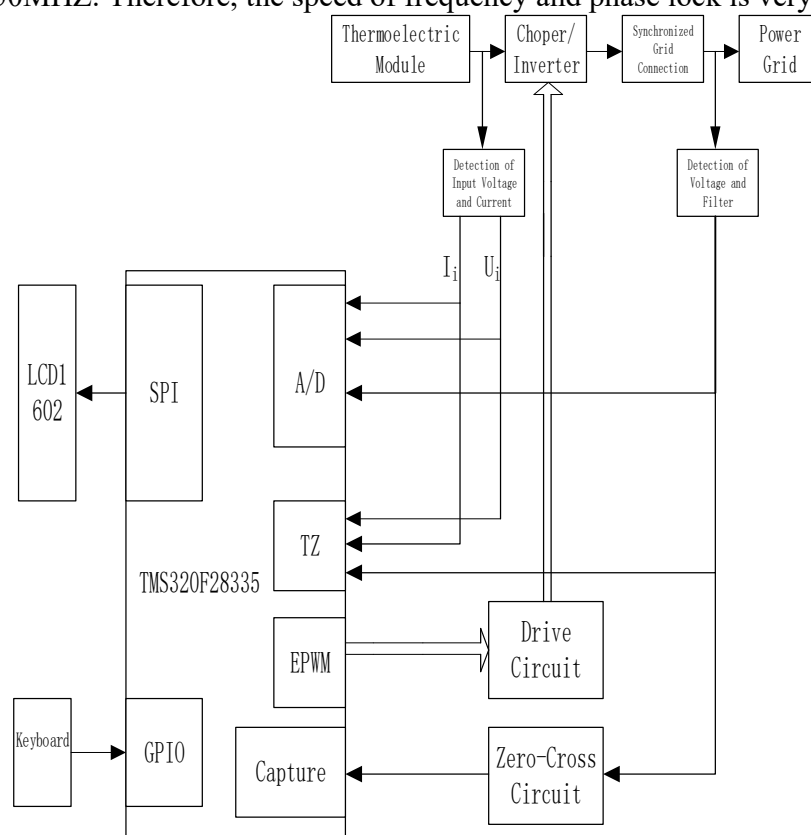

Figure 1. Block Diagram of Overall Design

2. Hardware and software design of TGS

2.1. SPWM mathematical principles

The sinusoidal pulse width modulation (SPWM) is used as the control strategy to drive EPWM module of TMS320F28335 to generate AC power. The basic control principle is shown in the Figure 2. U_c is the carrier signal. And U_r is the modulated signal.
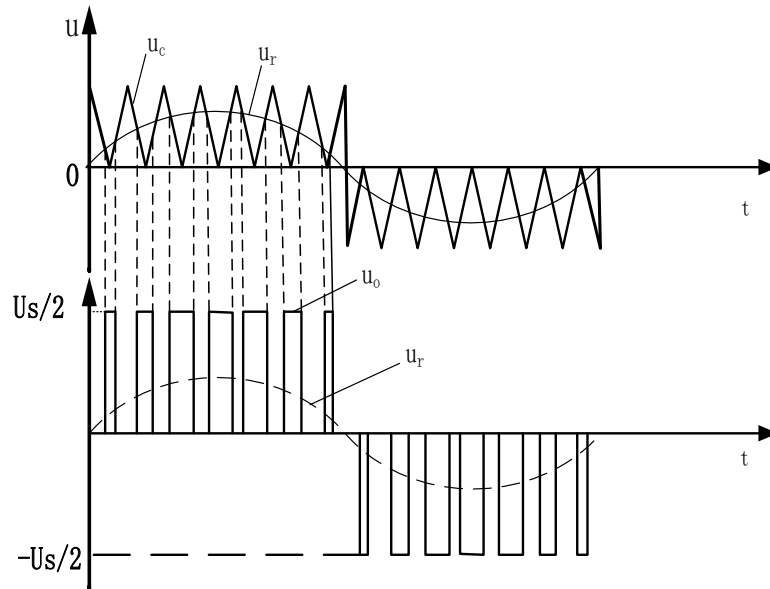
Figure 2. SPWM Modulation Waveform

The equation (1) is used to calculate the width of a single pulse $t_{p\omega}$.

$$t_{pw} = \frac{T_s}{2}(1 + M \sin \omega t_1) \tag{1}$$

$$M = \frac{|U_r|}{|U_c|} \tag{2}$$

ω is the power grid angular frequency.

$$T_s = \frac{1}{F_c * N} = \frac{T_c}{N} \tag{3}$$

T_s is the carrier period. F_c is the frequency of the power grid. The value is around 50HZ. N is the carrier ratio. The value is 400 in this design. T_C is the period of the power grid which can be measured by the CAPTURE module of TMS320F28335. Therefore, the system can adjust the output SPWM pulse according to the measured value of T_C. Then the purpose of locking frequency and phase can be achieved [7-10].

2.2. Full bridge circuit
Figure 3 is the full bridge circuit. SPWM signal which is used to drive the circuit to generate sinusoidal waveform of the same frequency and phase as the power grid [11-14].
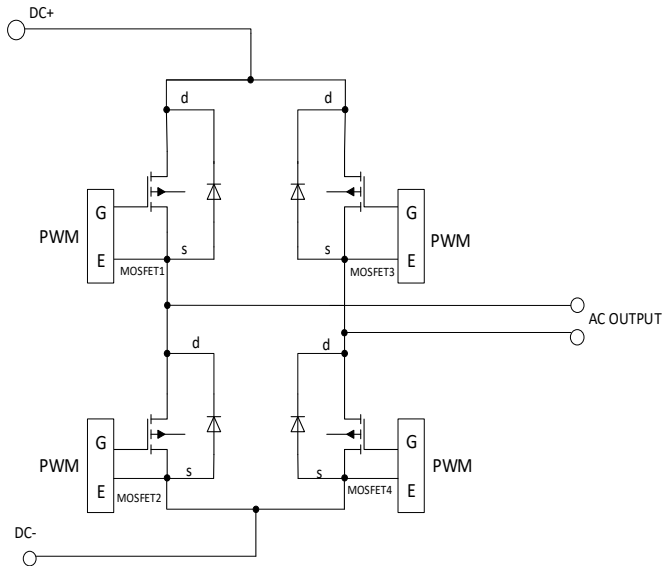
Figure 3. Full Bridge Circuit

2.3. Flow chart of EPWM interrupt service program

Figure 4 is the flow chart of EPWM interrupt service program. It describes the details of the process of the EPWM.
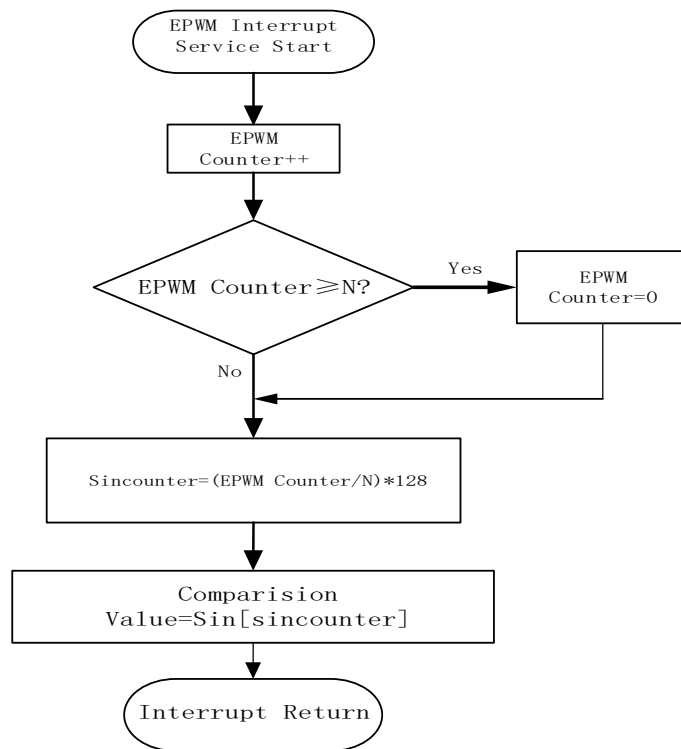

Figure 4. Flow chart of EPWM interrupt service program

3. Signal acquisition and FIR filter processing

The external signals are converted to analog signals and then the analog signals are converted into digital signals. The digital signal will be sent to the DSP by A/D conversion. After filtering in the TMS320F28335, the signal can be used to calculate frequency and phase.

As a typical digital filter, the finite length pulse response (FIR) filter has non recursive structure. It can ensure the strict linear phase and frequency characteristics at the same time. And it is stable and easy to use in hardware. The equation (4) is shown as following.

$$y(n) = \sum_{k=0}^{N-1} h(k)x(n-k) \tag{4}$$

The transmission function is shown as equation (5).

$$H(Z) = \sum_{k=0}^{N-1} h(k)Z^{-k} \tag{5}$$

Where N is the order of the filter, its structural form is shown in the Figure 5.
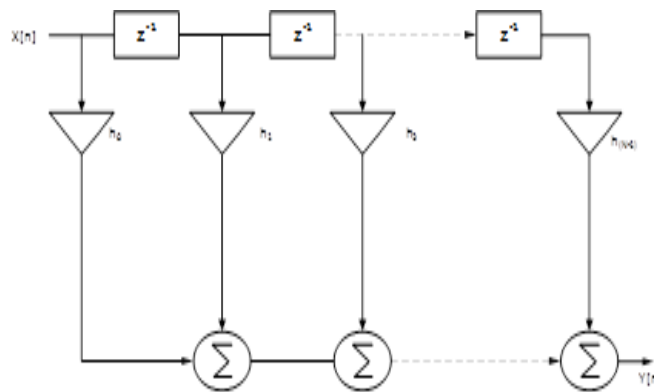

Figure 5. FIR Schematic Diagram

The coefficients of FIR can be calculated by MATLAB software.
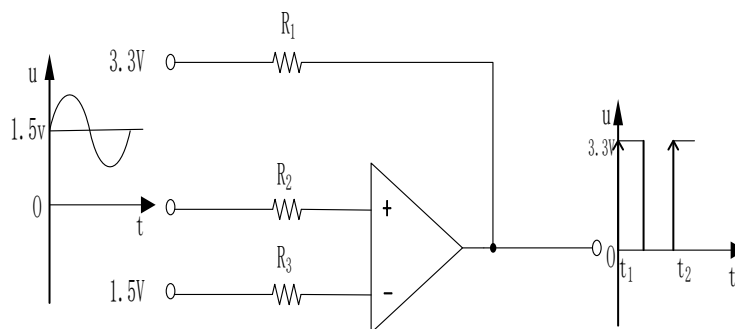
4. AC zero-crossing circuit diagram

Figure 6. AC Zero-crossing Circuit Diagram

As shown in the Figure 6, the square waveform which is generated by zero-crossing comparison circuit is connected to the CAPTURE pin of TMS320F28335. The time difference between the two rising edges of the square waveform is T_c.

$$T_c = t_2 - t_1 \tag{6}$$

T_c is the period of the power grid signal. The frequency of power grid is as shown in the equation (7).

$$F_c = 1/T_c \tag{7}$$

And the difference between the rising edge of the power grid and invertor is the phase difference between them.

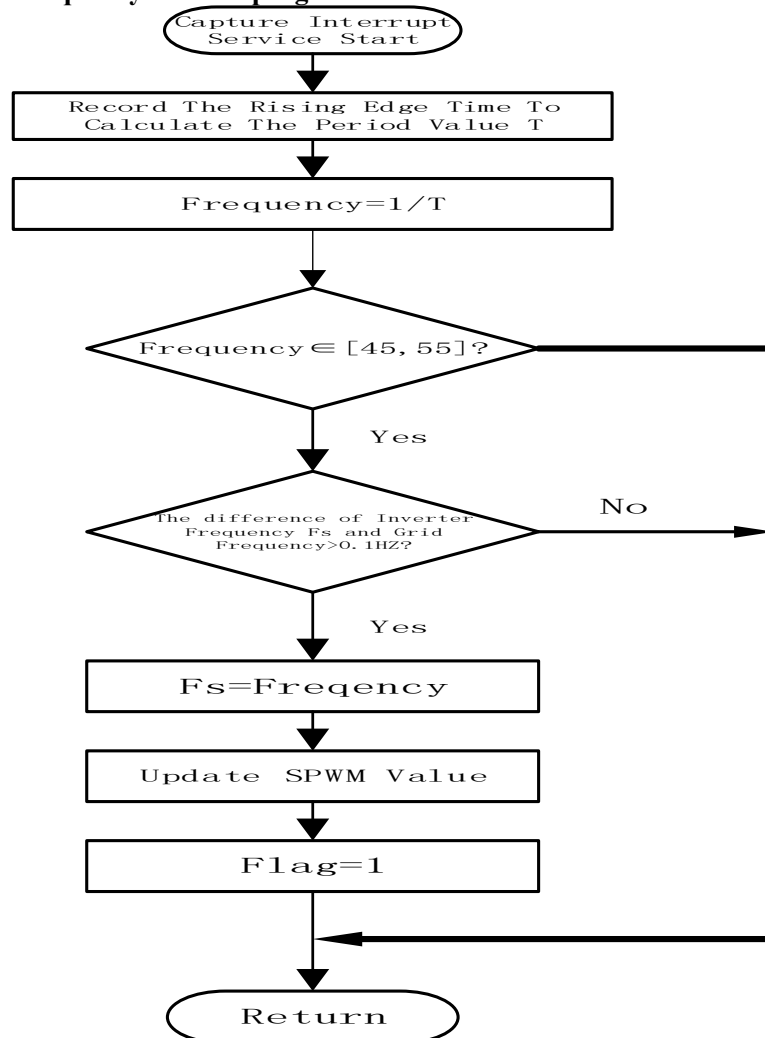## 5. Flow chart of frequency lock subprogram

Figure 7. Flow Chart of Frequency Locking Subprogram

As shown in the Figure7, the frequency locking has been described. The detection and processing method of phase-lock is similar to that of frequency-lock. The initial phase of SPWM waveform will be directly modified after calculating the phase difference. In fact, the phase-lock program determines the position of the first pulse in the SPWM waveform. And the frequency-lock program completes the following pulse of all the pulses in a period of SPWM waveform. Therefore, the system can accomplish frequency-lock and phase-lock at the same time in one period [15-16].

6. Experimental Result and Conclusion

The experiment has been executed. Figure 8 is the waveform of pin1 and pin 3 of the Boost Circuit's MOSFET. Figure 9 is the waveform of pin1 and pin 3 of the inverter's MOSFET. Figure 10 is the final comparing waveform of frequency and phase lock.
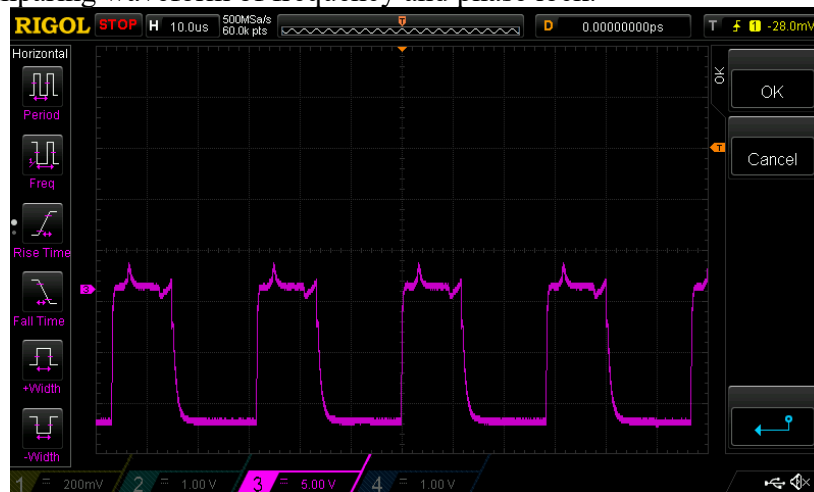

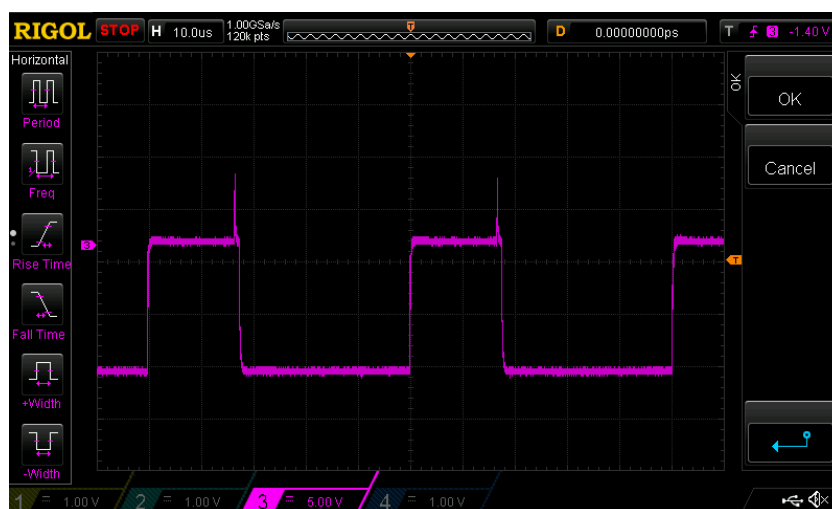**Figure 8.** Waveform of Pin1 and Pin 3 of the Boost Circuit's MOSFET

Figure 9. Waveform of Pin1 and Pin 3 of Inverter's MOSFET

Figure 10. Waveform of Frequency and Phase Lock

In the Figure10, the blue waveform is the power grid sampling signal. And the Yellow waveform is the inverter output signal. These two waveforms have the same frequency and phase. The experimental results show that the design of fast frequency-lock and phase-lock is feasible.

References

[1]   Xu W, Deng J, Xie C and Quan S 2017 A new type of power supply system for automotive thermoelectric power generation research on optimal control strategy of weak hybrid power *International Conference on Industrial Informatics - Computing Technology, Intelligent Technology, Industrial Information Integration (ICIICII), Wuhan,* 286-89.

[2]   Takahashi M and Deng M. 2013 Experimental studies on power control of semiconductor thermoelectric power generation system Proceedings of the 2013 *International Conference on Advanced Mechatronic Systems, Luoyang,* 182-86.

[3]   Chen Yaai, Liu Jingdong, Zhou Jinghua and Li Jin 2013 Research on the control strategy of PV grid-connected inverter upon grid fault *International Conference on Electrical Machines and Systems (ICEMS), Busan,* 2163-67.

[4]   Alatawi KS, Almasoudi FM and Matin M A 2017 Highly efficient GaN-based single-phase transformer-less PV grid-tied inverter *North American Power Symposium (NAPS), Morgantown, WV,* 1-6.

[5]   Dhara S, Hota A, Jain S and Agarwal V 2018 A novel single-phase t-type pv inverter with improved dc utilization *IEEE International Conference on Power Electronics, Drives and Energy Systems (PEDES), Chennai, India,* 1-5.

[6]   Zulkifli SA, Ariffn MAM., Sean TC and Sobri NHM 2018 Control model development using

TMS320F28335 microcontroller for high rated inverter and DC motor drive application, *5th IET International Conference on Clean Energy and Technology (CEAT2018), Kuala Lumpur,* 1-5.

[7] Guedouani R, Fiala B and Boucherit M S 2017 Implementation of multi-carrier PWM using a DSP TMS320F28335 application to series multicellular single-phase inverter *2017 10th International Conference on Electrical and Electronics Engineering (ELECO), Bursa,* 1424-29.

[8] Stanzione S, Van Liempd C, and Van Hoof C 2013 Integrated asynchronous high-voltage DC-DC buck converter for energy harvesting applications *Electron. Lett.* **49** 210–11

[9] Shah H A, Shah S K and Patel R. 2015 DSP based PWM generation for high switching frequency voltage source inverter *2015 International Conference on Communications and Signal Processing (ICCSP), Melmaruvathur,* 0517-20.

[10] Zhong Q C and Weiss G 2011 Synchronverters: inverters that mimic synchronous generators *IEEE Transactions on Industrial Electronics* **58** 1259–67.

[11] Kim J and Kim C 2013 A DC–DC boost converter with variation-tolerant MPPT technique and efficient ZCS circuit for thermoelectric energy harvesting applications *IEEE Transactions on Power Electronics* **28** 3827-33

[12] Hsin C, Wu M and Wang W 2019 Thermoelectric devices by half-millimeter-long silicon nanowires arrays *IEEE Transactions on Nanotechnology* **18** 921-24

[13] Dong Y, Ding J, Huang J, Xu L and Dong W 2015 Investigation of thermal electric generation system inverter MPPT efficiency test *platform International Conference on Renewable Power Generation (RPG 2015), Beijing,* 1-4.

[14] Rocabert J, Luna A, Blaabjerg F, Rodri X and Guez P 2012 Control of power converters in AC microgrids *IEEE Trans. Power Electron* **27** 4734–49

[15] Balaguer I J, Lei Q, Yang S, et al. Control for grid-connected and intentional islanding operations of distributed power generation *IEEE Transactions on Industrial Electronics* **58** 147-57

[16] Guan M, Xu Z, and Chen H 2011 Control and modulation strategies for modular multilevel converter based HVDC system *37th Annu. Conf. IEEE Ind. Electronics Soc* 849–54.